Int J Adv Manuf Technol (2017) 90:3001–3011
DOI 10.1007/s00170-016-9604-2

ORIGINAL ARTICLE

Process parameter determination of the axial-pushed incremental rolling process of spline shaft

Min-Chao Cui[1] · **Sheng-Dun Zhao**[1] · **Chao Chen**[1] · **Da-Wei Zhang**[1] · **Yong-Yi Li**[1]

Received: 12 June 2016 / Accepted: 10 October 2016 / Published online: 26 October 2016

Abstract The process parameters of the axial-pushed incremental rolling process are studied in this paper to solve the problems in present production process of spline shaft. Firstly, the principle of the axial-pushed incremental rolling process is introduced. Based on the material of 42CrMo, the simplified finite element models of the process are established up. Then, the effects of process parameters and the material flow behavior during the process are investigated by finite element analysis (FEA). After that, the reasonable process parameters during the novel process (die angle 9°, feed speed 0.5 mm s^{-1}, and speed of rolling die 25 r min^{-1}) are determined to meet a good balance between the forming force, product precision, and processing efficiency. To verify the determined parameters, validation tests with the blank material 42CrMo were carried out on an axial-pushed incremental rolling equipment. The experimental results (tooth shape and forming force) show a good agreement with FEA results. Through the dimension measurement, the addendum and root circle diameters of formed spline shafts are 51.61, 51.72, and 51.66 mm and 48.66, 48.78, and 48.69 mm, respectively. The formed spline shafts with the determined process parameters reach to the requirement of direct use (required addendum circle diameter 51.56~51.75 mm, required root circle diameter 48.5~48.7 mm). Finally, the feasibility of the determined process parameters with other materials (no. 20 and no. 45 steel) is investigated. The dimensions of the formed spline shafts just slightly deviate from the theoretical value. This problem is solved by adjusting the feed speed and the speed of rolling die. Therefore, the determined process parameters of the axial-pushed incremental rolling process are usable for the production of spline shaft.

Keywords Axial-pushed incremental rolling process · Spline shaft · Process parameters · FEA · Experiments

1 Introduction

Spline shafts are usually applied as the key parts to transmit motion or torque between shafts in mechanical equipment, and the superiorities of spline shafts can be summarized as follows: high reliability, high connection strength, convenient assembly, and compact structure, etc. Thus, the various superiorities of spline shafts bring a huge application and demand of spline shafts in the industries such as automobile, engineering machinery, ship, and aerospace. For example, a standard car contains more than 30 spline shafts, and the installed positions of spline shafts have transmission, differential, clutch, etc. In addition, the modern industry brings higher manufacturing requirement to the productive efficiency and performance of spline shaft. Therefore, it is urgent to study an advanced manufacturing process for the spline shaft with higher efficiency and performance.

Currently, the studies of the plastic forming process of spline and gear become ever more active for the superiorities such as lower cost, high product quality, higher productivity, and saving of materials. Klepikov and Bodrov [1] draw a conclusion that the cold plastic forming process of spline shafts is a better way in mass production by their applied research. Li et al. [2] have studied an open-die warm extrusion process of spline shafts. In their study, the effects of main process parameters on tooth filled quality and forming loads are investigated by finite element method (FEM). Altinbalik

✉ Min-Chao Cui
cuiminchao@163.com

[1] School of Mechanical Engineering, Xi'an Jiaotong University, Xi'an, Shaanxi, China

and Ayer [3] have investigated a forward extrusion process of clover section from different billet diameters. Zou et al. [4] have designed an optimal die profile via integrating FEM during hot extrusion process. The surface load distributes on die profile surface more uniformly, and then, the service life of die in hot extrusion process is improved. Zhang et al. [5] have established up the mathematical models of contact area and tooth curves in the two- or three-die spline rolling process. In order to solve the bulging problem during cold extrusion of spline shaft, Huang and Fu [6] have proposed a method of adding a guide length upon entrance section of the die in the die designing. Kondo et al. [7] have proposed a tooth crest divided flow method of precision cold forging process.

Zhang and Zhao [8] have proposed a new way for forming shafts having thread and spline by rolling with two round dies. Zhang et al. [9] also have studied the method of initial phase adjustment for dies before spline rolling. The work provided a theoretical basis for the experimental rolling process of splined shafts. Weisz-Patrault et al. [10] have proposed a new roll gap friction sensor for cold rolling process, which enables to evaluate contact stresses with very short computation times, compatible with real-time interpretation. Using a slip-line field method, Zhang et al. [11] investigated the rolling force and torque during spline shaft rolling process with round dies. Liu et al. [12] have carried out the experimental research on forming parameters for spline shaft rolling process with round dies.

Based on the previously mentioned research works, a novel axial-pushed incremental rolling process of spline shaft is proposed to try to promote the application of plastic forming process in manufacturing. There are some important process parameters (for example, feed in velocity, die angle of entrance section, and rotational speed of dies) of axial-pushed incremental rolling process, and FEA is widely used to determine the process parameters. In previous works, FEA or FEM was proved to be an effective method to understand forming mechanism and determine the process parameters. Kamouneh et al. [13] declared that diagnosis of quality problems and proposing possible solutions to the problems in helical gear rolling process with flat dies can be carried out by FEM. Yang et al. [14] have studied the blank size effects on the uniformity of strain and temperature distributions during hot rolling of titanium alloy large rings by finite element (FE) modeling. Domblesky and Feng [15] have studied the effects of forming parameters on the thread rolling with flat dies by using FEM. Hua et al. [16] have investigated the size effects of rolls on the radial–axial ring rolling process based on a valid 3D FE model. Kao et al. [17] developed an integrated CAD/CAM/CAE system to design the flat dies in taper-tipped screw rolling process. Tieu et al. [18] have investigated the influence of cold rolling reduction on the deformation behavior and crystallographic orientation development by FEM simulation. Carvalho-Resende et al. [19] have developed an elastoplastic constitutive model by numerical study for sheet steel forming. Li et al. [20] have studied the cold rolling process for double groove ball-section ring by finite element modeling and simulation.

In this paper, an axial-pushed incremental rolling process of spline shaft is studied. It is a novel metal forming process during which the blank is pushed into the rolling dies incrementally and the material in the surface layer is formed to needed shape. The material flow behavior and optimum process parameters during the process are investigated by FEA. Based on the specific axial-pushed incremental rolling equipment, the experimental research is carried out by the authors. Then, the experiments with the determined parameters are carried out on the equipment and the forming precision is verified.

2 Principle of the axial-pushed incremental rolling [21]

The principle of the axial-pushed incremental rolling process is shown in Fig. 1a; the system is mainly made up of by blank, back-drive center, and three rolling dies. The rolling dies were installed along the circumferential direction evenly. Figure 1b shows the structure of the rolling die; each rolling die contains die angle and correction part along the axial direction. The die angle part preformed for spline shaft, and the correction part formed and adjusted the tooth profile. The back-drive center could confirm that the initial phase of the three dies is suitable and ensure that the speed stays the same because it has the same parameters with spline shaft.

3 Determination of the process parameters by FEA

3.1 Finite element modeling and simulation parameters

Based on the principle of the process, the simplified finite element models of the axial-pushed incremental rolling

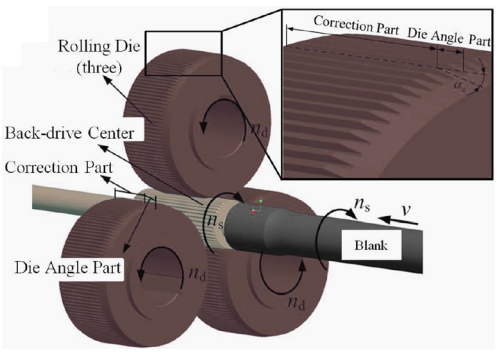

Fig. 1 Diagram of the principle of the axial-pushed incremental rolling process

process are established up, as shown in Fig. 2a. The blank structure, constraints, and grid are shown in Fig. 2b. Along the axial direction, the blank contains three sections: (a) tooth profile section, (b) transition section, and (c) connection section. The length of the tooth profile section is 32 mm. The connection section can be regarded as no deformation, so the constraints of no displacement in all directions are applied in connection section. Additionally, in order to increase the precision of simulations, local mesh refinement is applied in the surface within the depth of 1.5 mm.

The material of the blank is set as 42CrMo steel (American Grade: AISI 4140), which is used for spline shaft widely in automobile industry. The constitutive equation of 42CrMo at room temperature is obtained by compression tests on INSTRON® universal mechanical testing machine. And the Johnson–Cook model is employed to express the constitutive equation of 42CrMo, as shown in Eq. 1.

$$\sigma = \left(414 + 542.34\varepsilon_{\mathrm{p}}^{0.2878}\right)\left(1 + 0.04618\ln\dot{\varepsilon}\right) \quad (1)$$

The simulation parameters of FEA are as follows. The mesh type is selected as tetrahedral mesh, and the remeshing criterion is set as global remeshing (interference depth 0.7, relative). The blank temperature and environment temperature are 20 °C. The shear-based friction model is applied between the blank and the dies, and the friction factor is set as 0.12 according to the user guide of DEFORM®.

In order to improve the simulation efficiency and ensure the authenticity and accuracy of the results, some assumptions are made for finite element models. There is no ductile fracture, and the material develops no anisotropy during deformation. Both Bauschinger effects and elastic recovery of material are not taken into account. The effects of gravity and inertia force of the blank itself are neglected. The finite element models with the previously mentioned assumptions are similar to real-life situations of axial-pushed incremental rolling process.

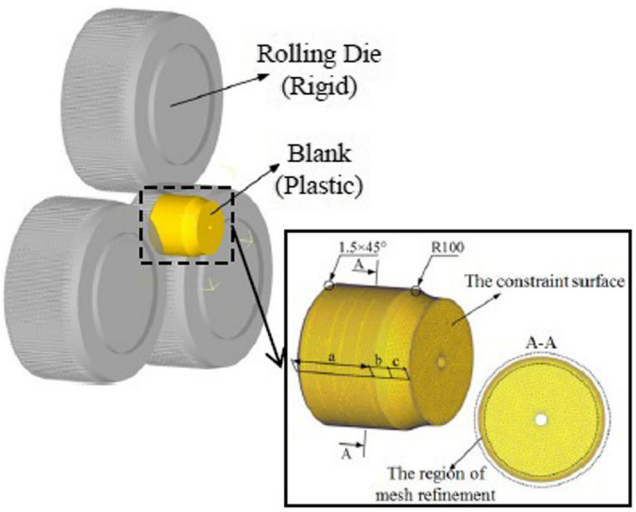

Fig. 2 Diagram of the finite element models

3.2 The determination of the die angle α_e

The effects of the die angle are investigated in this paper. Different die angles (4°, 8°, 10°, 12°, 16°, 20°) are selected to simulate the axial-pushed incremental rolling process of spline shaft, and the results are analyzed, respectively. The other simulation conditions are selected as follows: the speed of rolling die is 20 r min^{-1}, the speed of blank is 60 r min^{-1}, and the axial feed speed is 1.5 mm s^{-1}. Figure 3 shows the rolling forming process with different α_e. When the rolling cycles $N_r = 5$, the rolling dies only make a shallow indentation on the blank of spline shaft with 4° die angle and the indentation is easy to produce dislocation in the next rolling cycle. But the rolling dies make a complete tooth profile on the blank with 20° die angle. When the rolling cycles $N_r = 5$, the rolling dies just begin to make complete tooth profile with 4° die angle. But in the situation of 10° and 20°, the length of complete tooth profile is already 6.7 and 8.8 mm. Thus, it can be seen that the increase of die angle can improve the efficiency and accuracy of the rolling process.

Figure 4 shows the tendency of the axial and radial rolling force with different die angles. With the increase of α_e, the rising rate of the axial and radial rolling force increases, the maximum axial rolling force increases, but the maximum radial rolling force decreases. When α_e increases from 4° to 20°, the maximum axial force increases from about 1.5 to 2.4 kN, but the maximum radial force decreases from about 23.9 to 7.4 kN. Excessive axial rolling force is negative for axial infeed, but excessive radial rolling force is negative for rolling accuracy. Therefore, the determination of die angle should consider the axial and radial rolling force at the same time.

The die angle has a significant impact for the equivalent stress distribution of material in preformation area. The larger the die angle, the higher the actual rolling speed and deformation rate. Figure 5 shows the equivalent stress distributions on the section in preformed area (axial distance 20 mm), and the stress distributions are greatly different with different α_e. The equivalent stress distribution is basically identical when α_e ranges from 4° to 8° (Fig. 5a, b), and the equivalent stress on the surface of tooth root area is about 1300 MPa. When the α_e is 4°, the deformation and flow of material mainly occurred along the radial inward direction and the two-side direction, and the flow of the material in axial direction is less. But when α_e ranges from 8° to 16°, the deformation and flow of the material increased along the axial direction. These make the flow resistance of material decrease. Thus, the equivalent stress in the surface layer of spline shaft reduced (Fig. 5c–e). When α_e is 20° (Fig. 5f), the increase of deformation rate led to the equivalent stress rise in the surface layer of spline shaft

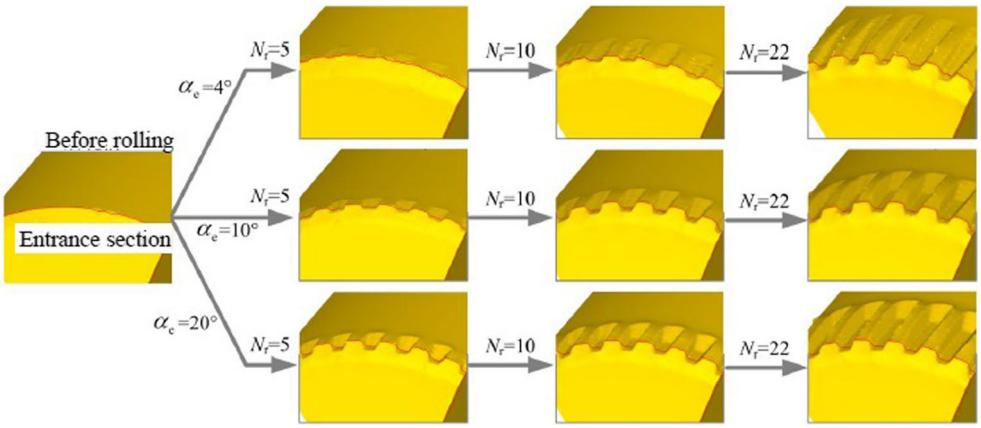

Fig. 3 The rolling forming process with different die angles

(the maximum equivalent stress is 1564 MPa on the surface of tooth root area). Therefore, the die angle should be appropriate to ensure the sufficient plastic deformation and material flow in the rolling process.

Figure 6 shows the equivalent strain distribution on the section (axial distance 20 mm) of the preformed area with different die angles. The depth of plastic deformation area decreases with α_e increasing, which indicates that the degree of plastic deformation accumulation reduced. When α_e ranges from 4° to 8° (Fig. 6a, b), the equivalent strain is almost evenly distributed in the tooth profile and root area of spline shaft. The equivalent strain in the center of tooth profile slightly declines, and the equivalent strain on the surface of tooth root area obviously increases. When α_e is bigger than 10°, especially 20°, the equivalent strain is mainly distributed on the surface of tooth profile and root, and it obviously declines in the center of tooth profile and the bottom of tooth profile and root (Fig. 6c–f). Therefore, a smaller α_e can improve the degree of plastic deformation accumulation and distribution uniformity. And then, the smaller α_e can improve the effect of work hardening, surface quality, and fatigue strength of tooth profile.

Figure 7 shows the distribution of the material flow displacement on the section (axial distance 20 mm) of preformation area. The displacement of material flow mainly distributes in the tooth profile and root area, and the maximal value appears in the top of the tooth profile and the surface of the tooth root. When α_e is 16° and 20° (Fig. 7e, f), the displacement of the material obviously increases in the tooth profile and root area. The reason for this phenomenon is that the increase of α_e leads to enhancement of actual rolling speed and axial flow of material.

Figure 8 shows the comparison of material flow displacement of the preformed area with different α_e in different directions. With the α_e increasing, (1) at the same radial (r_p), the displacement along the radial direction in tooth profile and root area is basically equal; (2) the direction of material flow in tooth profile area is inward radial direction, and the displacement increases with r_p; (3) the direction of material flow in tooth root area is outward radial direction, and the displacement also increases with r_p; (4) in tooth profile area, the displacement along the axial direction slightly increases with the α_e increasing, but it decreases with the increase of r_p; and (5) in tooth root area, the displacement along the axial direction obviously increases with the α_e increasing, and it also increases sharply with the increase of r_p (especially in the surface layer of the tooth root area r_p = 24.25 mm, the axial displacement of material flow increases rapidly when α_e is bigger than 10°). Thus, it can be seen that during the preformation process, smaller α_e can improve the behavior of material flow along the outward radial direction in tooth profile area and inhibit the behavior of material flow along the axial direction in toot profile and root area, which is beneficial to the increase of tooth height of spline shaft.

In summary, the increase of α_e is beneficial to the efficiency and accuracy of the rolling process, but it is not advantage for the axial rolling force, the material flow, the degree of plastic deformation accumulation, and the distribution uniformity. As a result, the optimum α_e is determined as 9° considering the effects of die angle on plastic deformation accumulation, material flow and rolling force.

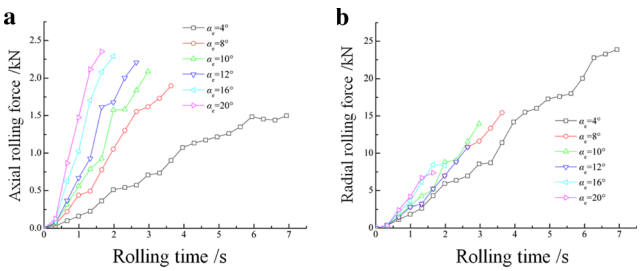

Fig. 4 The change trends of rolling force with different die angles: **a** axial rolling force and **b** radial rolling force

3.3 The determination of the feed speed ν

In order to investigate the effects of feed speed and determine the reasonable speed value, the axial-pushed incremental

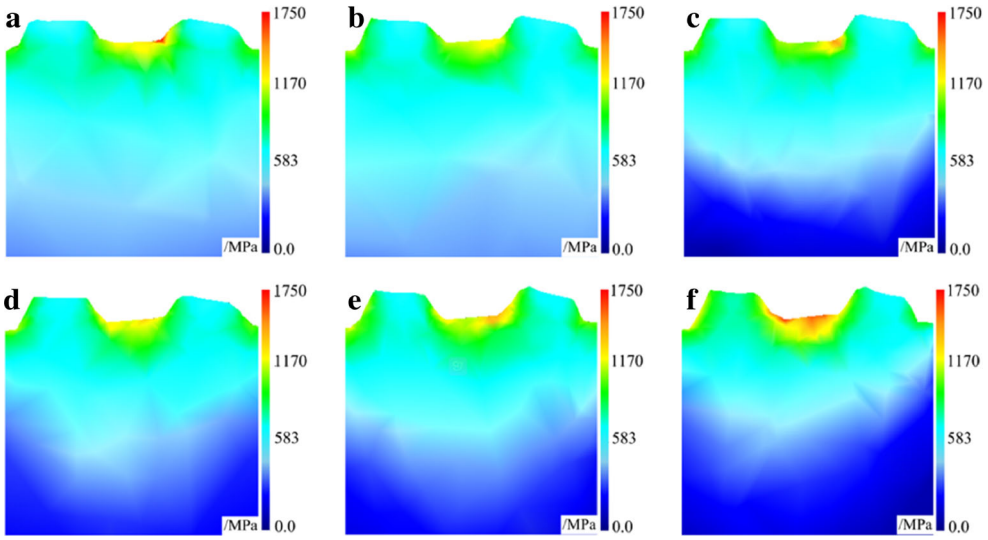

Fig. 5 The equivalent stress distribution on the section in preformed area with different die angles: **a** 4°, **b** 8°, **c** 10°, **d** 12°, **e** 16°, and **f** 20°

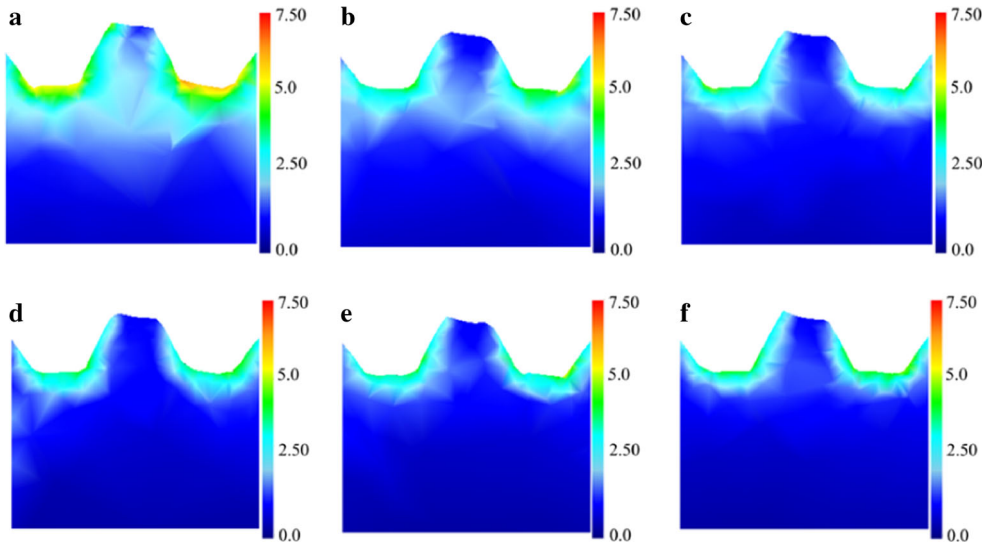

Fig. 6 The equivalent strain distribution on the section of the preformed area with different die angles: **a** 4°, **b** 8°, **c** 10°, **d** 12°, **e** 16°, and **f** 20°

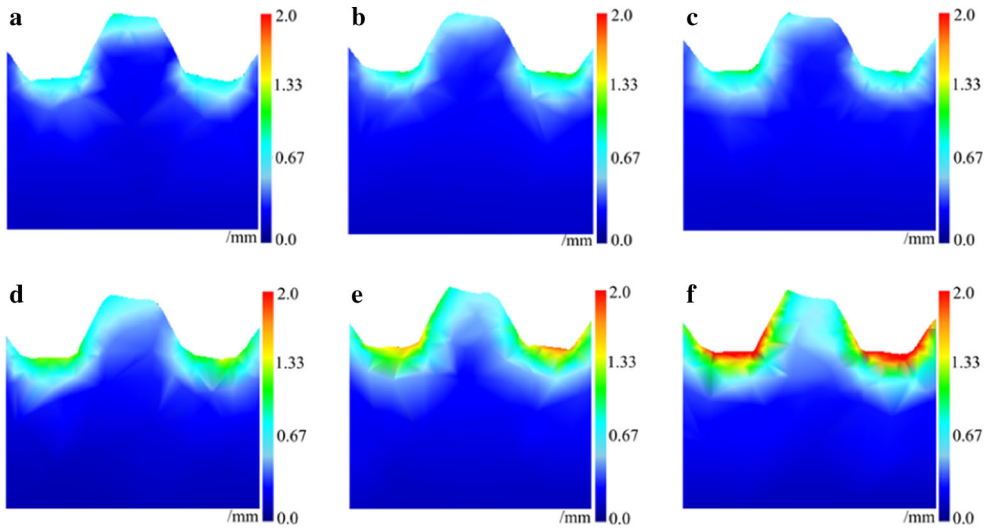

Fig. 7 The distribution of the material flow displacement on the section of preformed area: **a** 4°, **b** 8°, **c** 10°, **d** 12°, **e** 16°, and **f** 20°

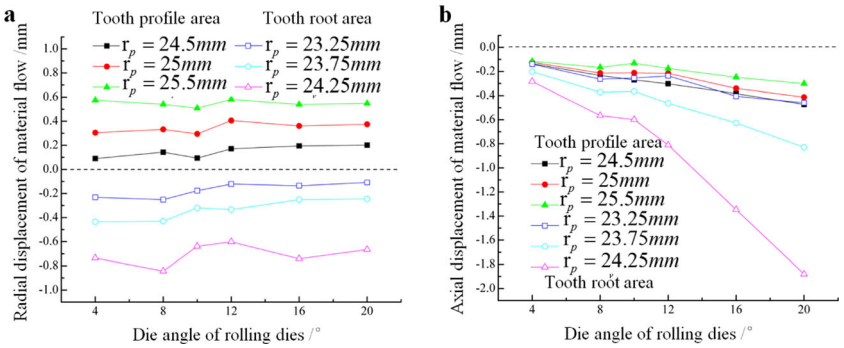

Fig. 8 The comparison of material flow displacement of preformed area with different die angles in different directions: **a** radial direction and **b** axial direction

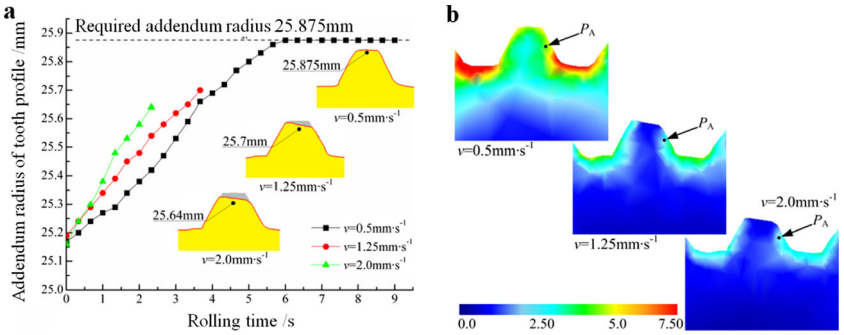

Fig. 9 The simulation results with different feed speeds: **a** the variation of addendum radius when pre rolling and **b** the distribution of equivalent strain with different feed speeds in preformed area

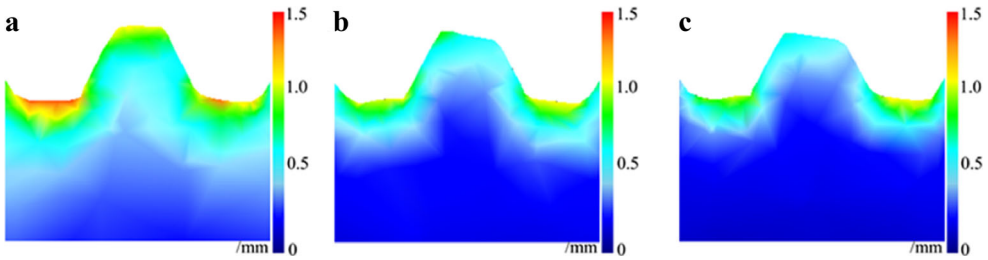

Fig. 10 The distribution of the material flow displacement with different feed speeds ν: **a** 0.5, **b** 1.25, and **c** 2 mm s^{-1}

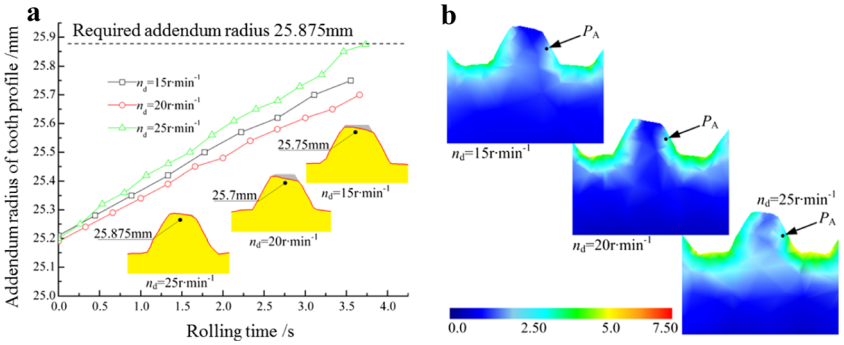

Fig. 11 The simulation results with different rotation speeds of rolling dies: **a** the variation of addendum radius when prerolling and **b** the distribution of equivalent strain with different feed speeds in preformed area

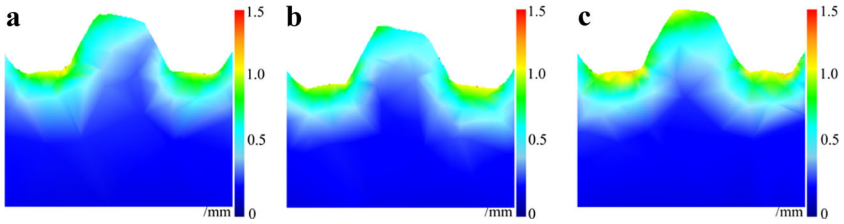

Fig. 12 The distribution of the material flow displacement with different rotation speeds of rolling dies n_d: **a** 15, **b** 20, and **c** 25 r min^{-1}

rolling process is simulated with different feed speeds ν (0.5, 1.25, and 2 mm s^{-1}) and the results are shown in Fig. 9. The other simulation conditions are set as follows: the die angle α_e is 9°, the speed of rolling die is 20 r min^{-1}, and the speed of blank is 60 r min^{-1}. According to Fig. 9, with the increasing of ν, the forming speed of tooth profile increases, but the radius of addendum decreases obviously after preformation. When the feed speed is 0.5, 1.25, and 2 mm s^{-1}, the radius of addendum is 25.875, 25.7, and 25.64 mm, respectively, as shown in Fig. 10a (only when the feed speed is 0.5 mm s^{-1}, the radius of addendum consistent with the requirement). As a result, the smaller ν can increase the cycles of preformation and is favorable to the increase of tooth height (the area of rolling in one cycle is small, so the accumulation degree of plastic deformation is higher).

Figure 9b shows the distribution of equivalent strain with different ν in the preformed area. The equivalent strain in tooth profile and root area decreases obviously as ν increases. For example, when the feed speed is 0.5, 1.25, and 2 mm·s^{-1}, the equivalent strain at P_A (depth 0.25 mm) is 4.802, 2.047, and 1.956, respectively. The reduction of equivalent strain indicates that the accumulation degree of plastic deformation decreases during the preformation process (the effect of work hardening weakens, and then, the fatigue strength of tooth profile lowers). In addition, the reduction of ν can increase the correction rolling cycles of rolling dies and improve the surface quality of the tooth profile and root area.

Figure 10 shows the distribution of the material flow displacement on the section (axial distance 20 mm) in preformation area with different feed speeds. The displacement in tooth profile and root area decreases as the feed speed increases, and the value is bigger in tooth profile area. This phenomenon indicates that the increase of feed speed leads to more drastic plastic deformation (material flow is not sufficient and the displacement decreases). Then, the radius of addendum remarkably reduces after preforming.

As a result, the enhancement of feed speed suppresses the accumulation of plastic deformation and the behavior of the material flow. In order to improve the surface quality and structural property of the formed spline shaft, ν should not be too large (the reasonable ν value can be determined as 0.5 mm s^{-1} in actual rolling process).

3.4 The determination of the speed of rolling die n_d

The simulations with different speeds of rolling die n_d (15, 20, and 25 r min^{-1}) were submitted to calculate. The speeds of blank are set as 45, 60, and 75 r min^{-1} accordingly. The feed speed is set as 1.25 mm s^{-1} in order to decrease the computation time, and the die angle α_e is set as 9°. Figure 11 shows the variation of the addendum radius and the distribution of the equivalent stress with different rotation speeds of rolling dies n_d. With the increasing n_d, the rotating period of the spline shaft shortens, the preforming cycles of rolling dies increase, and the deformation area of one cycle decreases. Thus, the accumulation degree of plastic deformation is higher during the preforming process. As shown in Fig. 11a, the radius of addendum reached the required radius (25.875 mm) after preforming when n_d is equal to 25 r min^{-1}. But when it is 20 or 15 r min^{-1}, the radius of addendum slightly decreases after preforming. This phenomenon could be explained as follows: the deformation area of one cycle increases as n_d decreases, and the material plastic deformation and flow are insufficient. Thus, the radius of addendum decreases when n_d is 20 or 15 r min^{-1}.

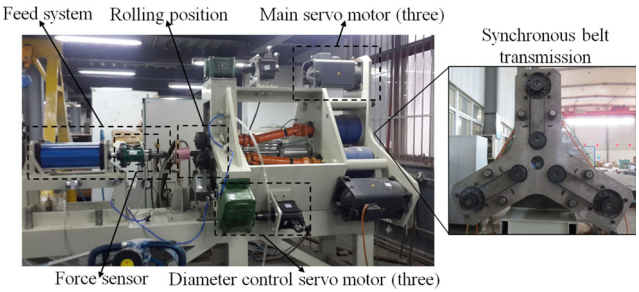

Fig. 13 The axial-pushed incremental rolling equipment

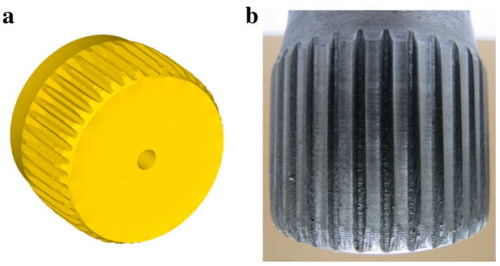

Fig. 14 The comparison of formed spline shaft with 42CrMo: **a** FEA result and **b** experimental result

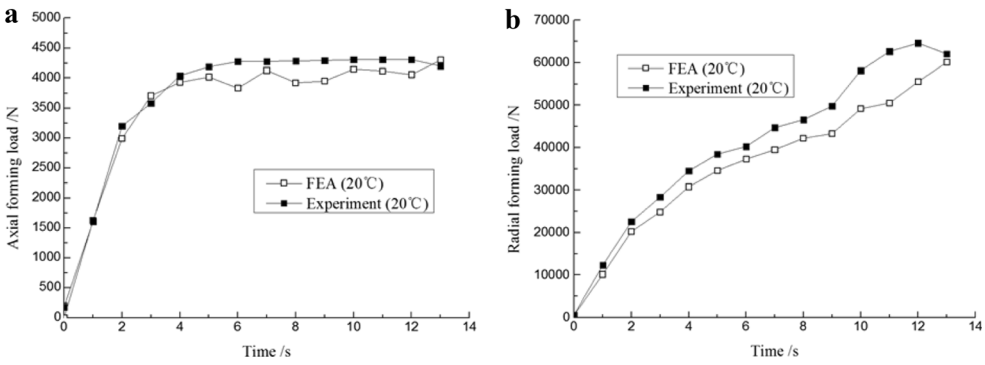

Fig. 15 The comparison of forming load results by FEA and experiments: **a** axial forming load and **b** radial forming load

Figure 11b shows the distribution of equivalent strain with different n_d after preforming. The equivalent strain obviously increases with n_d. For example, when n_d is 15, 20, and 25 r min^{-1}, the equivalent strain of P_A is 1.642, 2.047, and 2.655, respectively. In addition, after 10 cycles of correction rolling, the equivalent strain of P_A increases to 1.642, 2.047, and 2.655, respectively (improved 88.1, 91.6, and 127.6 %, respectively). This result reveals that the increase of n_d can deepen the plastic deformation accumulation in tooth profile and root area.

Figure 12 shows the distribution of the material flow displacement on the section (axial distance 20 mm) in the preformed area with different n_d. The material flow displacement of tooth profile and root area increases with n_d.

As a result, the increase of n_d can increase the cycles of preforming rolling and correction rolling. Thus, the deformation area of one cycle decreases and the degree of plastic deformation accumulation increases (the effect of work hardening is more obvious). However, the oversize speed of rolling die is difficult for the rolling equipment design. In order to obtain the forming quality as good as possible, the reasonable n_d value can be determined as 25 r min^{-1} in actual rolling process.

4 Experimental verification of the determined process parameters

4.1 Experimental preparation

Based on the principle in Sect. 2, an axial-pushed incremental rolling equipment was designed, manufactured, and assembled as shown in Fig. 13.

Then, the experiments of the axial-pushed incremental rolling process of spline shaft with the determined process parameters are carried out and the forming precision is investigated.

4.2 The experimental verification of finite element models

In order to validate the finite element models in Sect. 3, the corresponding experiments were conducted on the rolling equipment. The final results of FEA (die angle 9°, feed speed 0.5 mm s^{-1}, speed of rolling die 25 r min^{-1}) were adopted for the experimental conditions. The experimental blanks are machined with 42CrMo steel according to the shape of FEA blank model, and the mineral oil is used for lubrication between the surfaces of blank and rolling dies. Figure 14 shows the final formed spline shafts by FEA and experiment with the same conditions. The tooth number is the same, and the tooth shape shows a good agreement.

In addition, the finite element forming load results, which were calculated by FEA, are compared with the experimental results, as shown in Fig. 15. Both the axial loads and radial loads have a good consistency with the experimental load data. Therefore, the previously mentioned comparisons indicate that the finite element models and analysis in Sect. 3 are credible.

4.3 Experimental results

Figure 16 shows the formed spline shaft with 42CrMo steel. It can be seen that the tooth number of formed spline shaft is accurate and the tooth profile is equally distributed, undistorted, and smooth.

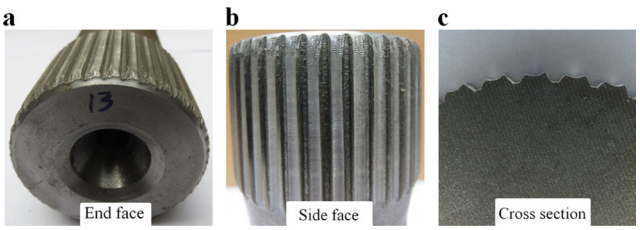

Fig. 16 Formed spline shafts with 42CrMo: **a** end face, **b** side face, and **c** cross section

Table 1 Parameters of the formed spline shaft with 42CrMo and the theoretical value

Project		Parameters			
		Tooth number	Addendum circle diameter (mm)	Root circle diameter (mm)	Base tangent length (mm)
Theoretical value		40	$51.75^{0}_{-0.19}$(h6)	$48.7^{0}_{-0.2}$	$24.746^{-0.04}_{-0.08}$
Experimental value	42CrMo sample 1	40	51.61	48.66	24.680
	42CrMo sample 2	40	51.72	48.78	24.793
	42CrMo sample 3	40	51.66	48.69	24.703

Then, the formed spline shafts by the axial-pushed incremental rolling process are measured, respectively, and the main parameters are compared with the theoretical value in Table 1. The formed spline shafts with the determined process parameters show a good shape, and all of the measured dimensions meet the theoretical value. Therefore, the determined process parameters of the axial-pushed incremental rolling process are available for the production of spline shaft and the formed spline shafts have reached the requirement of direct use.

4.4 The feasibility investigation on other materials

The previously mentioned analysis and experiments are based on the material of 42CrMo, and the final experimental results are satisfactory. Further, the feasibility on other materials is investigated in order to promote the application of the axial-pushed incremental rolling process with the determined process parameters. The no. 20 steel and no. 45 steel, which are commonly used in the present spline shaft production, are selected to experiment (the other experimental conditions are the same as Sect. 4.3), and Fig. 17 shows the shape of the formed spline shafts. As well, the formed shafts are measured respectively, and the results are listed in Table 2. The formed spline shafts also showed a good tooth shape, and the dimensions just slightly deviated from the theoretical value (the results are very close to the theoretical value because the optimal die angle makes a good balance between deformation accumulation and axial material flow). The reason for dimension deviation can be explained as follows: the material flow displacement is affected by the material properties, but the experimental conditions are determined by FEA based on the material of 42CrMo.

This problem can be solved by slightly adjusting the feed speed ν and the speed of rolling die n_d (decrease the feed speed or increase the speed of rolling die or both). The further experiments are also carried out, and the formed spline shafts are satisfactory. Therefore, the determined process parameters in this paper can be used for the spline shaft production with no. 20 and no. 45 steel after a small adjustment.

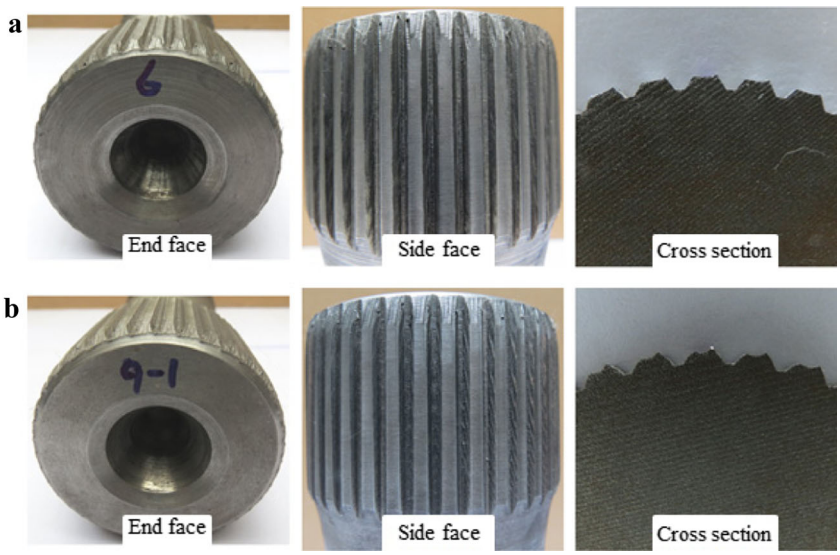

Fig. 17 The formed spline shaft with other materials: **a** no. 20 steel and **b** no. 45 steel

Table 2 Parameters of the formed spline shaft with other materials and the theoretical value

Project		Parameters			
		Tooth number	Addendum circle diameter (mm)	Root circle diameter (mm)	Base tangent length (mm)
Theoretical value		40	$51.75^{0}_{-0.19}$(h6)	$48.7^{0}_{-0.2}$	$24.746^{-0.04}_{-0.08}$
Experimental value	No. 20 sample 1	40	51.73	49.20	25.017
	No. 20 sample 2	40	51.64	49.03	24.964
	No. 20 sample 3	40	51.74	48.87	24.773
	No. 45 sample 1	40	51.67	49.32	25.183
	No. 45 sample 2	40	51.58	48.82	24.951
	No. 45 sample 3	40	51.62	48.65	24.732

5 Conclusion

Through the FEA and experimental verification on the axial-pushed incremental rolling process, the conclusions are listed as follows:

1. The deformation and material flow during the axial-pushed incremental rolling process of spline shaft only occur in the surface layer of the blank. The process parameters (die angle α_e, feed speed ν, and speed of rolling die n_d) have significant effects on the rolling process of spline shaft.
2. Based on the FEA on the rolling process with 42CrMo steel, the increase of α_e is beneficial to the efficiency and accuracy of the rolling process, but it is not advantage for the axial rolling force, the material flow, the degree of plastic deformation accumulation, and the distribution uniformity. Thus, an optimum die angle of rolling dies is established as 9° considering the effects of die angle on the axial-pushed incremental rolling process.
3. The FEA results demonstrate that the increase of feed speed is adverse to the accumulation of plastic deformation and the behavior of the material flow. However, an extreme feed speed is not available in the actual production because of poor efficiency. A reasonable feed speed value is determined as 0.5 mm s^{-1} to obtain the enough surface quality and structure property.
4. The bigger rotation speed of rolling die can increase the cycles of preforming rolling and the degree of plastic deformation accumulation. However, it is disadvantage for the rolling equipment design. Thus, a reasonable rotation speed value is determined as 25 r min^{-1} to obtain the forming quality as good as possible.
5. The experimental verification is carried out on the axial-pushed incremental rolling equipment, and the combination of the determined process parameters (die angle 9°, feed speed 0.5 mm·s^{-1}, speed of rolling die 25 r min^{-1}) is adopted for the experimental conditions. The formed spline shafts show a good agreement with FEA results, and the measurement results show that the dimension of formed spline shafts reached the requirement. Thus, the determined process parameters of the axial-pushed incremental rolling process are available for the production of spline shaft with 42CrMo steel.
6. The feasibility investigation on the commonly used materials of spline shaft (no. 20 steel and no. 45 steel) is discussed. The measurement results of the formed spline shafts just slightly deviated from the theoretical value. This problem is solved by slightly adjusting the feed speed ν and the speed of rolling die n_d (decrease the feed speed or increase the speed of rolling die or both).

Compliance with ethical standards

Funding The authors gratefully acknowledge the contribution of the following: National Natural Science Foundation of China for Key Program (Grant No. 51335009) and Shaanxi Province Natural Science Foundation of China (Grant No. 2014JQ7273).

References

1. Klepikov VV, Bodrov AN (2003) Precise shaping of splined shafts in automobile manufacturing. Russ Eng Res 23:37–40
2. Li YY, Zhao SD, Fan SQ, Yan GH (2013) Study on the material characteristic and process parameters of the open-die warm extrusion process of spline shaft with 42CrMo steel. J Alloys Comp 571: 12–20
3. Altinbalik T, Ayer Ö (2008) A theoretical and experimental study for forward extrusion of clover sections. Mater Des 29:1182–1189
4. Zou L, Xia JC, Wang XY, Hu GA (2003) Optimization of die profile for improving die life in the hot extrusion process. J Mater Process Technol 142:659–664
5. Zhang DW, Li YT, Fu JH (2008) Tooth curves and entire contact area in process of spline cold rolling. Chin J Mech Eng 21:94–97

6. Huang ZH, Fu PF (2001) Solution to the bulging problem in the open-die cold extrusion of a spline shaft and relevant photo plastic theoretical study. J Mater Process Technol 114:185–188
7. Kondo K, Ohga K (1995) Precision cold die forging of a ring gear by divided flow method. Int J Mach Tools Manufact 35:1105–1113
8. Zhang DW, Zhao SD (2014) New method for forming shaft having thread and spline by rolling with round dies. Int J Adv Manuf Technol 70:1455–1462
9. Zhang DW, Zhao SD, Wu SB, Zhang Q (2015) Phase characteristic between dies before rolling for thread and spline synchronous rolling process. Int J Adv Manuf Technol 81:513–528
10. Weisz-Patrault D, Maurin L, Legrand N, Ben Salem A, Ait Bengrir A (2015) Experimental evaluation of contact stress during cold rolling process with optical fiber Bragg gratings sensors measurements and fast inverse method. J Mater Process Technol 223:105–123
11. Zhang DW, Li YT, Fu JH, Zheng QG (2009) Rolling force and rolling moment in spline cold rolling using slip-line field method. Chin J Mech Eng 22:688–695
12. Liu ZQ, Song JL, Qi HP, Li YT, Li XD (2010) Parameters and experiments on the precision forming process of spline cold rolling. Appl Mech Mater 34–35:646–650
13. Kamouneh AA, Ni J, Stephenson D, Vriesen R, Degrace G (2007) Diagnosis of involute metric issues in flat rolling of external helical gears through the use of finite-element models. Int J Mach Tools Manuf 47:1257–1262
14. Yang H, Wang M, Guo LG, Sun ZC (2008) 3D coupled thermo-mechanical FE modeling of blank size effects on the uniformity of strain and temperature distributions during hot rolling of titanium alloy large rings. Comp Mater Sci 44:611–621
15. Domblesky JP, Feng F (2002) Two-dimensional and three-dimensional finite element models of external thread rolling. Proc Instn Mech Engrs Part B, Journal of Engineering Manufacture 216: 507–517
16. Zhou G, Hua L, Qian DS (2011) 3D coupled thermo-mechanical FE analysis of roll size effects on the radial–axial ring rolling process. Comp Mater Sci 50:911–924
17. Kao YC, Cheng HY, She CH (2006) Development of an integrated CAD/CAE/CAM system on taper-tipped thread-rolling die-plates. J Mater Process Technol 177:98–103
18. Deng GY, Tieu AK, Si LY, Su LH, Lu C, Wang H, Liu M, Zhu HT, Liu XH (2014) Influence of cold rolling reduction on the deformation behaviour and crystallographic orientation development. Comp Mater Sci 81:2–9
19. Carvalho-Resende T, Balan T, Bouvier S, Abed-Meraim F, Sablin SS (2012) Numerical investigation and experimental validation of a plasticity model for sheet steel forming. Model Simul Mater Sci 21: 008–015
20. Li LY, Li X, Liu J, He Z (2013) Modeling and simulation of cold rolling process for double groove ball-section ring. Int J Adv Manuf Technol 69:1717–1729
21. Cui MC, Zhao SD, Zhang DW, Chen C, Fan SQ, Li YY (2016) Deformation mechanism and performance improvement of spline shaft with 42CrMo steel by axial-infeed incremental rolling process. Int J Adv Manuf Technol. doi:10.1007/s00170-016-8997-2